Inorganic Chemistry

Article

pubs.acs.org/IC

# Synthesis, Structures, And Magnetic Behavior of New Anionic Copper(II) Sulfate Aggregates and Chains

Andrew D. Burrows,*[†] Mary F. Mahon,[†] Viorica M. Sebestyen,[†] Yanhua Lan,[‡] and Annie K. Powell[‡,§]

[†]Department of Chemistry, University of Bath, Claverton Down, Bath BA2 7AY, U.K.

[‡]Institut für Anorganische Chemie, Karlsruhe Institute of Technology, Engesserstrasse 15, D76131 Karlsruhe, Germany

[§]Institute of Nanotechnology, Karlsruhe Institute of Technology, Hermann-von-Helmholtz Platz 1, 76344 Eggenstein-Leopoldshafen, Germany

Supporting Information

**ABSTRACT:** The reaction between $CuSO_4 \cdot 5H_2O$ and $[NMe_2H_2]Cl$ in *N*,*N*′-dimethylformamide (DMF) at 95 °C yielded green crystals of $(NMe_2H_2)_4[Cu_6O_2(SO_4)_6(DMF)_4]$ **1**. The discrete $[Cu_6(\mu_4\text{-}O)_2(\mu_3\text{-}SO_4)_4(\mu_2\text{-}SO_4)_2(DMF)_4]^{4-}$ anions present in **1** contain two edge-sharing $Cu_4(\mu_4\text{-}O)$ tetrahedra, with the copper(II) centers bridged by sulfato ligands. These anions are linked into a two-dimensional network through hydrogen bonds involving the dimethylammonium cations. When the reaction was carried out in the absence of $[NMe_2H_2]Cl$, yellow-green crystals of $(NMe_2H_2)_4[Cu_6O_2(SO_4)_6(DMF)_2]$ **2** were obtained. The anions in **2** contain similar $Cu_6O_2(SO_4)_6$ aggregates to those in **1**, though these differ in terms of the copper(II) coordination geometries. In addition, the anions in **2** are linked into chains through bridging sulfato ligands. The $Cu_6O_2(SO_4)_6$ aggregates observed in **1** and **2** are related to those present in the rare copper sulfate mineral fedotovite, $K_2Cu_3O(SO_4)_3$, and in common with this mineral both **1** and **2** decompose in the presence of moisture. The reaction between $CuSO_4 \cdot 5H_2O$ and $[NMe_2H_2]Cl$ in DMF at room temperature gave $(NMe_2H_2)[Cu_2(OH)(SO_4)_2(H_2O)_2]$ **3**, the structure of which contains triangular $Cu_3(OH)(SO_4)$ units that share vertices to form tapes. Magnetic measurements revealed that **1** and **3** are both spin-canting metamagnetic systems. Field-induced responses were observed below 5 K, with the critical field indicating metamagnetic behavior from antiferromagnetic to ferromagnetic equal to 110 Oe for both compounds.

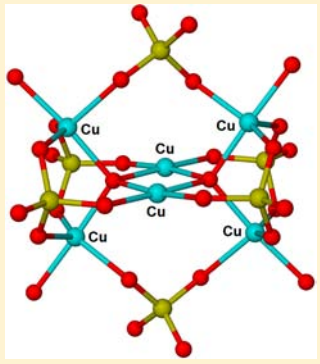


## INTRODUCTION

Copper(II) sulfate is one of the first compounds encountered by many budding chemists, with the distinctive blue color of the pentahydrate readily recognizable. It is used in a wide range of school experiments including crystal growing, dehydration, and copper plating. Copper(II) sulfate also has many industrial applications including use as a fungicide, algaecide, and molluscicide,[1−3] and as an activator in the concentration by froth flotation in the mining industry.[4] A wide variety of copper(II) sulfate minerals are also known in which the copper(II) and sulfate ions occur together with anions such as hydroxide,[5,6] or cations such as sodium or potassium.[7]

Copper(II) sulfate is often used in combination with multidentate *N*-donor ligands to form coordination networks. Since sulfate is generally a better ligand than nitrate or perchlorate, reactions with $CuSO_4 \cdot 5H_2O$ are more likely to lead to mixed-ligand products than analogous reactions with $Cu(NO_3)_2$ or $Cu(ClO_4)_2$. For example, reactions of $CuSO_4 \cdot 5H_2O$ with pyridine-substituted tetrazoles were recently reported to lead to open framework coordination networks containing both sulfate and pyridyl-tetrazolate ligands,[8] whereas reactions involving chelating ligands have afforded sulfate-bridged dimers.[9] Sulfates can link copper(II) centers into aggregates such as hexamers[10] and tetramers,[11] that can themselves be further cross-linked into extended structures. Coordination networks can even be formed in the absence of additional ligands, and a number of anionic copper(II) sulfate structures have been reported in which the charges on the anions are balanced by included ammonium cations.[12]

In this paper we report the synthesis and characterization of three new copper(II) sulfate compounds, in which anionic copper-sulfate aggregates and chains are charge balanced by dimethylammonium ions derived either from the hydrolysis of the *N*,*N*′-dimethylformamide (DMF) solvent[13] or from the addition of $[NMe_2H_2]Cl$. These compounds have been crystallographically characterized as $(NMe_2H_2)_4[Cu_6O_2(SO_4)_6(DMF)_4]$ **1**, $(NMe_2H_2)_4[Cu_6O_2(SO_4)_6(DMF)_2]$ **2**, and $(NMe_2H_2)[Cu_2(OH)(SO_4)_2(H_2O)_2]$ **3**, and the magnetic properties of **1** and **3** have also been investigated.

## EXPERIMENTAL SECTION

**General Procedures.** The reagents used for the syntheses were purchased commercially and used without further purification. The DMF was ACS reagent quality.

Powder X-ray diffraction patterns were recorded on a Bruker AXS D8 Advance diffractometer with copper K$\alpha$ radiation of wavelength 1.5418 Å at 298 K. DMF-saturated samples were placed in 0.5 mm

**Received:** July 9, 2012
**Published:** September 17, 2012

Table 1. Crystal Data and Structure Refinement Details for Compounds 1−3

| | 1 | 2 | 3 |
|---|---|---|---|
| chemical formula | $C_{20}H_{60}Cu_6N_8O_{30}S_6$ | $C_{14}H_{46}Cu_6N_6O_{28}S_6$ | $C_2H_{13}Cu_2NO_{11}S_2$ |
| $M$ (g mol$^{-1}$) | 1466.36 | 1320.17 | 418.33 |
| crystal system | monoclinic | triclinic | monoclinic |
| space group | $P2_1/n$ | $P\bar{1}$ | $P2_1/n$ |
| $a$/Å | 13.1050(3) | 8.5880(2) | 6.8990(1) |
| $b$/Å | 10.5140(2) | 10.6840(3) | 17.0780(4) |
| $c$/Å | 18.7530(5) | 12.8170(3) | 10.3860(3) |
| $\alpha$/deg | 90.00 | 106.496(1) | 90.00 |
| $\beta$/deg | 103.183(1) | 104.593(1) | 90.779(1) |
| $\gamma$/deg | 90.00 | 105.935(2) | 90.00 |
| unit cell volume/Å$^3$ | 2515.81(10) | 1012.49(4) | 1223.58(5) |
| temperature/K | 150(2) | 150(2) | 150(2) |
| $Z$ | 2 | 1 | 4 |
| no. of reflections measured | 39253 | 15974 | 22218 |
| no. of independent reflections | 5766 | 4615 | 2802 |
| $R_{int}$ | 0.1191 | 0.0492 | 0.0879 |
| final $R_1$ values ($I > 2\sigma(I)$) | 0.0582 | 0.0326 | 0.0389 |
| final $wR(F^2)$ values ($I > 2\sigma(I)$) | 0.1230 | 0.0760 | 0.0811 |
| final $R_1$ values (all data) | 0.0890 | 0.0450 | 0.0636 |
| final $wR(F^2)$ values (all data) | 0.1379 | 0.0813 | 0.0910 |
| goodness of fit on $F^2$ | 1.077 | 1.068 | 1.069 |

diameter Lindemann capillaries, and measured with a 2$\theta$ range of 3−60°. The step size was 0.016° with a time per step of 134.5 s. Simulated X-ray powder patterns were generated from single crystal data that were imported into PowderCell,[14] with the step size of 0.02° and time per step of 1.00 s.

Magnetic susceptibility measurements were obtained using a Quantum Design SQUID (superconducting quantum interference device) MPMS-XL susceptometer. This magnetometer works between 1.8 and 400 K for direct current (DC) applied fields ranging from −70 to 70 kOe. Measurements were performed on polycrystalline samples of **1** (33.0 mg) and **3** (36.7 mg). Alternating current (AC) susceptibility measurements were measured with an oscillating AC field of 3 Oe and AC frequencies at 1000 Hz. The magnetic data were corrected for the sample holder.

**Synthesis of $(NMe_2H_2)_4[Cu_6O_2(SO_4)_6(DMF)_4]$ 1.** $CuSO_4{\cdot}5H_2O$ (0.060 g, 0.24 mmol) and $[NMe_2H_2]Cl$ (0.013 g, 0.16 mmol) were dissolved with stirring in DMF (12 cm$^3$). The reaction mixture was placed in a 30 cm$^3$ thick-walled glass vial and heated at 95 °C for 24 h to yield tiny green crystals. The PXRD pattern of the product showed a good match with the pattern simulated from the X-ray single crystal structure (Supporting Information, Figure S1). The sample was carefully dried under a flow of nitrogen and stored in a sealed flask under nitrogen.

**Synthesis of $(NMe_2H_2)_4[Cu_6O_2(SO_4)_6(DMF)_2]$ 2.** $CuSO_4{\cdot}5H_2O$ (0.60 g, 2.4 mmol) was dissolved with stirring in DMF (12 cm$^3$). This solution was placed in a 30 cm$^3$ thick-walled glass vial and heated at 95 °C for 24 h. The powder X-ray diffraction pattern of the resultant tiny yellow-green crystals matches that simulated from the X-ray crystal structure (Supporting Information, Figure S2). The sample was carefully dried under a flow of nitrogen and stored in a sealed flask under nitrogen.

**Synthesis of $(NMe_2H_2)[Cu_2(OH)(SO_4)_2(H_2O)_2]$ 3.** $CuSO_4{\cdot}5H_2O$ (0.6 g, 2.4 mmol) and $[NMe_2H_2]Cl$ (0.13 g, 1.6 mmol) were dissolved with stirring in DMF (12 cm$^3$). This solution was placed in a vial and left undisturbed at room temperature. Turquoise crystals started to appear after a week, but the crystals were left in the mother liquor for a further two weeks after which they were harvested. The powder X-ray diffraction pattern of the product matches that simulated from the X-ray crystal structure (Supporting Information, Figure S3).

**X-ray Crystallography.** X-ray diffraction data on structures were collected on a Nonius Kappa CCD diffractometer, using Mo−K$\alpha$ radiation of wavelength 0.71073 Å at 150 K. Crystal data and details of the structural refinements are given in Table 1. The structures were solved using SHELXS-97 and refined using full-matrix least-squares in SHELXL-97.[15] The final refinements were generally straightforward. Unless noted below, all non-hydrogen atoms were refined anisotropically in the final least-squares run, and hydrogen atoms were included at calculated positions. In the structure of **2**, one of the dimethylammonium cations (that based on N(3)) was disordered in a 80:20 ratio. Only the major occupancy fragment atoms therein were refined anisotropically. Oxygen bound hydrogen atoms for **3** were located and refined at 0.98 Å from the relevant parent atoms.

## RESULTS AND DISCUSSION

Compounds **1** and **2** were initially obtained serendipitously from reaction mixtures containing copper(II) sulfate pentahydrate and dicarboxylic acids in DMF, though subsequently the presence of the dicarboxylic acid was found to be unnecessary. Compound **1** was prepared by heating a mixture of $CuSO_4{\cdot}5H_2O$ and $[NMe_2H_2]Cl$ in DMF at 95 °C for 24 h. Powder X-ray diffraction studies on the resulting tiny green crystals revealed that **1** is metastable, with the compound undergoing a series of structural changes over the course of a month. Compound **2** was prepared as tiny yellow-green crystals by heating $CuSO_4{\cdot}5H_2O$ in DMF at 95 °C for 24 h. As with **1**, compound **2** is metastable, undergoing a series of structural changes over several weeks, as witnessed by changes in the powder X-ray diffraction patterns. When water was added to the DMF solvent, the reaction gave a turquoise solid that was shown by powder X-ray diffraction to be $Cu_3(SO_4)(OH)_4$, which is the mineral antlerite.[16] Compound **3** was prepared from a mixture of $CuSO_4{\cdot}5H_2O$ and $[NMe_2H_2]Cl$ in DMF at room temperature, with the resultant turquoise crystals harvested after three weeks.

Compounds **1**−**3** are all moisture-sensitive, with **1** and **2** decomposing rapidly in the presence of water and **3** decomposing more slowly. These decompositions occur with absorption of water to form pastes and color changes to pale blue. The sensitivity of **1**−**3** prevented accurate microanalysis from being obtained, though in all cases the powder X-ray diffraction patterns of the DMF-saturated samples (Supporting


dx.doi.org/10.1021/ic301478x | Inorg. Chem. 2012, 51, 10983−10989

Information, Figures S1–S3) show a good correspondence to those simulated from the X-ray single crystal analyses (vide infra).

The crystal structure of $(NMe_2H_2)_4[Cu_6O_2(SO_4)_6(DMF)_4]$ **1** contains dimethylammonium cations and discrete $[Cu_6O_2(SO_4)_6(DMF)_4]^{4-}$ anions. The anions contain two edge-sharing $Cu_4(\mu_4\text{-}O)$ tetrahedra (Figure 1a), with the four triangular $Cu_3$ faces not involving the shared edge each capped by a $\mu_3$-sulfato ligand. Two $\mu_2$-sulfato ligands bridge between pairs of nonshared vertices on the two tetrahedra, and each copper center not involved in edge-sharing is also coordinated to a DMF ligand (Figure 1b). Hence the anion can be represented as $[Cu_6(\mu_4\text{-}O)_2(\mu_3\text{-}SO_4)_4(\mu_2\text{-}SO_4)_2(DMF)_4]^{4-}$.

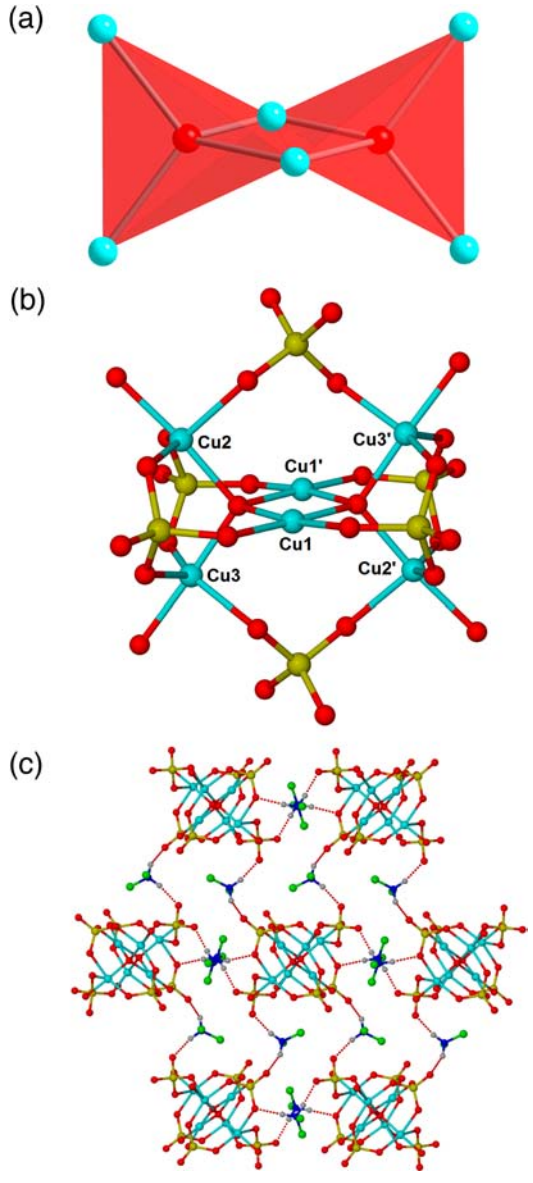


**Figure 1.** Structure of $(NMe_2H_2)_4[Cu_6O_2(SO_4)_6(DMF)_4]$ **1**, showing (a) the edge-sharing tetrahedra of the central $Cu_6$ aggregate, (b) the $[Cu_6O_2(SO_4)_6(DMF)_4]^{4-}$ anion, and (c) hydrogen bonding between the dimethylammonium cations and the $[Cu_6O_2(SO_4)_6(DMF)_4]^{4-}$ anions linking the aggregates into sheets. The nonoxygen atoms of the DMF ligands and all hydrogen atoms except those involved in hydrogen bonding have been removed for clarity. Primed atoms are generated by the symmetry operation $-x + 2, -y, -z$.

Selected bond lengths and angles for **1** are presented in Table 2. The $Cu_6O_2(SO_4)_6$ core is unusual, with the only previous example observed in the mineral fedotovite (vide infra).

**Table 2. Selected Bond Lengths (Å) and Bond Angles (deg) for 1**[a]

| | | | |
|---|---|---|---|
| Cu(1)–O(1)′ | 1.937(3) | Cu(1)–O(2) | 1.946(4) |
| Cu(1)–O(1) | 1.949(3) | Cu(1)–O(6)′ | 1.972(4) |
| Cu(2)–O(3) | 1.966(5) | Cu(2)–O(1) | 1.943(3) |
| Cu(2)–O(7) | 2.029(4) | Cu(2)–O(14) | 1.988(5) |
| Cu(3)–O(1) | 1.931(3) | Cu(2)–O(11)′ | 2.127(4) |
| Cu(3)–O(15) | 1.972(4) | Cu(3)–O(4) | 1.961(5) |
| Cu(3)–O(10) | 2.114(4) | Cu(3)–O(8) | 2.107(4) |
| | | | |
| O(1)′–Cu(1)–O(2) | 173.55(16) | O(1)′–Cu(1)–O(1) | 86.08(14) |
| O(2)–Cu(1)–O(1) | 93.59(16) | O(1)′–Cu(1)–O(6)′ | 96.46(15) |
| O(2)–Cu(1)–O(6)′ | 83.63(17) | O(1)–Cu(1)–O(6)′ | 176.64(15) |
| O(1)–Cu(2)–O(3) | 91.71(17) | O(1)–Cu(2)–O(14) | 174.55(18) |
| O(3)–Cu(2)–O(14) | 86.6(2) | O(1)–Cu(2)–O(7) | 95.27(15) |
| O(3)–Cu(2)–O(7) | 145.7(2) | O(14)–Cu(2)–O(7) | 83.29(19) |
| O(1)–Cu(2)–O(11)′ | 93.00(15) | O(3)–Cu(2)–O(11)′ | 119.7(2) |
| O(14)–Cu(2)–O(11)′ | 92.33(19) | O(7)–Cu(2)–O(11)′ | 93.46(18) |
| O(1)–Cu(3)–O(4) | 93.17(17) | O(1)–Cu(3)–O(15) | 176.64(16) |
| O(4)–Cu(3)–O(15) | 87.72(18) | O(1)–Cu(3)–O(8) | 91.49(14) |
| O(4)–Cu(3)–O(8) | 129.9(2) | O(15)–Cu(3)–O(8) | 85.46(16) |
| O(1)–Cu(3)–O(10) | 87.40(15) | O(4)–Cu(3)–O(10) | 143.8(2) |
| O(15)–Cu(3)–O(10) | 93.80(17) | O(8)–Cu(3)–O(10) | 86.15(16) |

[a]Primed atoms generated by the symmetry operation $-x + 2, -y, -z$.

The copper(II) centers involved in edge-sharing, Cu(1), have distorted square planar geometries, coordinated to two oxo and two $\mu_3$-sulfato ligands. The Cu(1)–O bond lengths lie between 1.937(3) and 1.972(4) Å, with *cis* O–Cu(1)–O bond angles between 83.63(17) and 96.46(15)°, and the Cu(1) center lies 0.072 Å from the mean plane defined by the four coordinating oxygen atoms. The Cu(1)···Cu(1)′ separation is 2.840(1) Å.

In contrast, Cu(2) and Cu(3), are both five-coordinate, with geometries between those expected for ideal square pyramidal and trigonal bipyramidal structures, as witnessed by $\tau$ values of 0.48 and 0.55 respectively.[17] Both of these copper(II) centers are coordinated to an oxo ligand, three sulfato ligands, and a DMF molecule. The DMF oxygen atom and oxo ligand are almost colinear [O(1)–Cu(2)–O(14) 174.55(18)°, O(1)–Cu(3)–O(15) 176.64(16)°], with the three oxygen atoms from the sulfato groups approximately coplanar.

In the crystal structure of **1**, the anions are linked into sheets by hydrogen bonding to the dimethylammonium cations (Figure 1c). The hydrogen bonds primarily involve the noncoordinated oxygen atoms of the sulfato ligands [O(12), O(13), O(9)] acting as acceptors, though notably the coordinated oxygen atom O(8) acts as an acceptor in place of the noncoordinated atom O(5), presumably for geometrical reasons. There are no strong interactions between the hydrogen-bonded sheets.


dx.doi.org/10.1021/ic301478x | *Inorg. Chem.* 2012, 51, 10983–10989

The crystal structure of $(NMe_2H_2)_4[Cu_6O_2(SO_4)_6(DMF)_2]$ **2** contains dimethylammonium cations and $[Cu_6O_2(SO_4)_6(DMF)_2]^{4-}$ anions. Selected bond lengths and angles are presented in Table 3. The structure of each

**Table 3. Selected Bond Lengths (Å) and Bond Angles (deg) for 2**[a]

| | | | |
|---|---|---|---|
| Cu(1)−O(1) | 1.952(2) | Cu(1)−O(1)′ | 1.990(2) |
| Cu(1)−O(2) | 1.999(2) | Cu(1)−O(8)′ | 1.972(2) |
| Cu(1)−O(10) | 2.214(2) | Cu(2)−O(1) | 1.9494(19) |
| Cu(2)−O(3) | 2.102(2) | Cu(2)−O(6) | 2.021(2) |
| Cu(2)−O(12)′ | 2.122(2) | Cu(2)−O(13)″ | 1.946(2) |
| Cu(3)−O(1) | 1.956(2) | Cu(3)−O(4) | 1.985(2) |
| Cu(3)−O(7) | 2.021(2) | Cu(3)−O(11) | 2.143(2) |
| Cu(3)−O(14) | 1.991(2) | | |
| | | | |
| O(1)−Cu(1)−O(8)′ | 169.88(9) | O(1)−Cu(1)−O(1)′ | 86.99(8) |
| O(8)′−Cu(1)−O(1)′ | 94.62(8) | O(1)−Cu(1)−O(2) | 94.90(8) |
| O(8)′−Cu(1)−O(2) | 82.22(9) | O(1)′−Cu(1)−O(2) | 172.19(8) |
| O(1)−Cu(1)−O(10) | 97.79(8) | O(8)′−Cu(1)−O(10) | 92.05(8) |
| O(1)′−Cu(1)−O(10) | 94.47(8) | O(2)−Cu(1)−O(10) | 92.78(8) |
| O(13)″−Cu(2)−O(1) | 168.09(9) | O(1)−Cu(2)−O(6) | 90.67(8) |
| O(13)″−Cu(2)−O(6) | 85.90(9) | O(1)−Cu(2)−O(3) | 93.21(8) |
| O(13)″−Cu(2)−O(3) | 81.94(9) | O(13)″−Cu(2)−O(12)′ | 92.62(9) |
| O(6)−Cu(2)−O(3) | 138.44(9) | O(6)−Cu(2)−O(12)′ | 121.35(8) |
| O(1)−Cu(2)−O(12)′ | 98.89(8) | O(3)−Cu(2)−O(12)′ | 98.86(9) |
| O(1)−Cu(3)−O(4) | 94.78(9) | O(1)−Cu(3)−O(14) | 171.96(9) |
| O(4)−Cu(3)−O(14) | 82.64(9) | O(1)−Cu(3)−O(7) | 94.10(8) |
| O(4)−Cu(3)−O(7) | 146.40(10) | O(14)−Cu(3)−O(7) | 84.09(9) |
| O(1)−Cu(3)−O(11) | 100.90(8) | O(4)−Cu(3)−O(11) | 110.28(9) |
| O(14)−Cu(3)−O(11) | 87.13(9) | O(7)−Cu(3)−O(11) | 99.69(9) |

[a]Primed atoms generated by the symmetry operation $-x + 2, -y, -z$. Double primed atoms generated by the symmetry operation $x + 1, y, z$.

$[Cu_6O_2(SO_4)_6(DMF)_2]^{4-}$ aggregate is broadly similar to the discrete $[Cu_6O_2(SO_4)_6(DMF)_4]^{4-}$ aggregates in **1**: two edge-sharing $Cu_4(\mu_4\text{-}O)$ tetrahedra are bridged by sulfato groups (Figure 2a). However, there are two significant differences between the aggregates in **1** and **2**. First, in **2**, the copper(II) centers involved in edge-sharing, Cu(1), exhibit square pyramidal geometry, with a $\tau$ value of 0.04, in contrast to the equivalent square planar centers in **1**. In **2**, Cu(1) is additionally coordinated to an oxygen atom from the sulfato ligand bridging between the copper(II) centers at the ends of the two tetrahedra. The axial contact, Cu(1)−O(10) 2.214(2) Å, is longer than those in the basal plane [1.952(2)−1.999(2) Å], but significantly shorter than the analogous nonbonded contact in **1** [Cu(1)···O(10) 2.666(4) Å].

The second significant change involves the number of coordinated DMF molecules. In **2** there are only two DMF ligands per anion, so Cu(2) is not solvated. Instead, it forms a Cu−O bond to a sulfato ligand from a neighboring aggregate [Cu(2)−O(13) 1.946(2) Å]. These interactions occur pairwise, and link the aggregates into chains that run along the *a* axis (Figure 2b). The coordination geometries of Cu(2) and Cu(3)

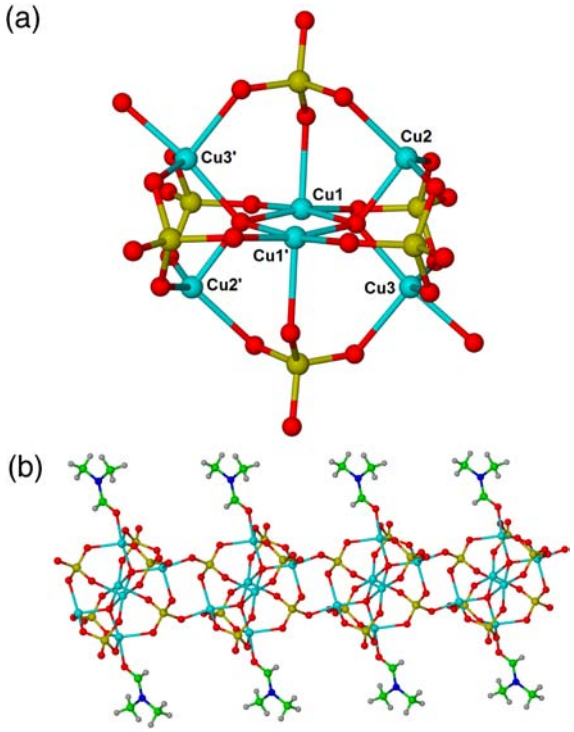


**Figure 2.** Structure of $(NMe_2H_2)_4[Cu_6O_2(SO_4)_6(DMF)_2]$ **2**, showing (a) the $[Cu_6O_2(SO_4)_6(DMF)_4]^{4-}$ anion, with the nonoxygen atoms of the DMF ligands removed for clarity, and (b) linking of the $[Cu_6O_2(SO_4)_6(DMF)_4]^{4-}$ aggregates into chains. Primed atoms are generated by the symmetry operation $-x + 2, -y, -z$.

are broadly similar to those of the equivalent atoms in **1**, being between those expected for ideal square pyramidal and trigonal bipyramidal geometries, as witnessed by $\tau$ values of 0.49 and 0.43, respectively. A consequence of these changes is that the $\mu_2$-sulfato ligand in **1** is replaced by a $\mu_4$-sulfato ligand in **2**.

As with **1**, hydrogen bonds are observed between the NH groups of the dimethylammonium cations and the sulfato oxygen atoms, with noncoordinated atoms O(5) and O(9) acting as hydrogen bond acceptors along with coordinated oxygen atoms O(6) and O(12). These hydrogen bonds link the one-dimensional coordination polymers into a three-dimensional network.

The crystal structures of **1** and **2** both have features in common with the structure of the rare copper sulfate mineral fedotovite, $K_2Cu_3O(SO_4)_3$,[18] which was first observed as a sublimate from the Tolbachik volcanic eruption in Kamchatka, Russia. Fedotovite contains the only previously reported example of the same $[Cu_6(\mu_4\text{-}O)_2(\mu_3\text{-}SO_4)_4(\mu_2\text{-}SO_4)_2]^{4-}$ building blocks (Figure 3a) as in **1**, though the $\mu_2$-sulfato groups bridge between these aggregates to form a two-dimensional coordination network (Figure 3b), which is linked into a three-dimensional structure by the potassium ions. Notably, like **1** and **2**, fedotovite has been observed to be unstable in air.

The crystal structure of $(NMe_2H_2)[Cu_2(OH)(SO_4)_2(H_2O)_2]$ **3** reveals a different solid-state architecture to those observed for **1** and **2**. In particular, **3** consists of triangular $Cu_3(\mu_3\text{-}OH)(\mu_3\text{-}SO_4)$ units that share vertices to form tapes running along the crystallographic *a* axis (Figure 4a). These tapes are reinforced by $\mu_4$-$SO_4$ ligands (Figure 4b). Selected bond lengths and angles for **3** are presented in Table 4.


dx.doi.org/10.1021/ic301478x | *Inorg. Chem.* 2012, 51, 10983−10989

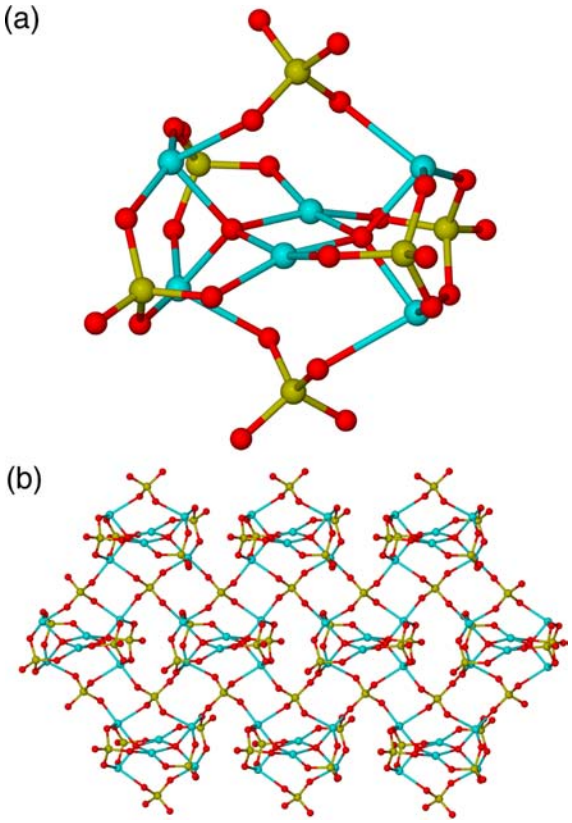


**Figure 3.** Structure of $K_2Cu_3O(SO_4)_3$, fedotovite, showing (a) the $Cu_6O_2(SO_4)_6$ aggregates, and (b) linking of the aggregates into sheets. Potassium cations have been removed for clarity.

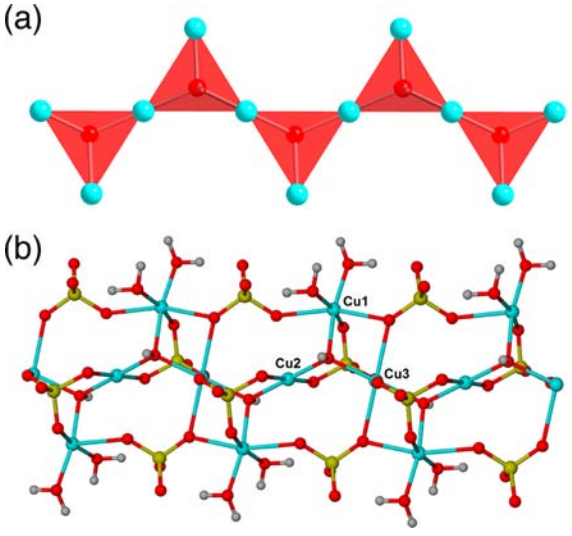


**Figure 4.** Structure of $(NMe_2H_2)[Cu_2(OH)(SO_4)_2(H_2O)_2]$ **3**, showing (a) the linked $Cu_3(OH)$ triangles, and (b) the $[Cu_2(OH)(SO_4)_2(H_2O)_2]^-$ tapes.

The copper(II) centers Cu(2) and Cu(3) link the triangles together into the tapes. These both exhibit tetragonally distorted octahedral geometries, and are coordinated to two hydroxyl oxygen atoms and two $\mu_3$-sulfato oxygen atoms in the equatorial plane, with two longer contacts to the $\mu_4$-sulfato oxygen atoms in the axial positions. The copper(II) center Cu(1) also has a tetragonally distorted octahedral geometry, and is coordinated to a hydroxyl group, two aqua ligands and a $\mu_3$-sulfato oxygen atom in the equatorial plane, and to two $\mu_4$-sulfato oxygen atoms in the axial positions.

**Table 4. Selected Bond Lengths (Å) and Bond Angles (deg) for 3[a]**

| | | | |
|---|---|---|---|
| Cu(1)−O(10) | 1.970(3) | Cu(1)−O(6) | 1.984(3) |
| Cu(1)−O(11) | 1.985(3) | Cu(1)−O(1) | 2.012(3) |
| Cu(1)−O(5)′ | 2.281(3) | Cu(1)−O(2) | 2.384(3) |
| Cu(2)−O(1) | 1.941(3) | Cu(2)−O(7) | 1.960(3) |
| Cu(3)−O(1) | 2.019(3) | Cu(3)−O(5)′ | 2.377(3) |
| Cu(3)−O(8) | 1.932(3) | | |
| O(10)−Cu(1)−O(6) | 86.65(12) | O(10)−Cu(1)−O(11) | 95.92(12) |
| O(6)−Cu(1)−O(11) | 166.99(12) | O(10)−Cu(1)−O(1) | 169.40(12) |
| O(6)−Cu(1)−O(1) | 91.00(11) | O(11)−Cu(1)−O(1) | 88.69(12) |
| O(10)−Cu(1)−O(5)′ | 90.85(11) | O(6)−Cu(1)−O(5)′ | 94.08(12) |
| O(11)−Cu(1)−O(5)′ | 98.62(12) | O(1)−Cu(1)−O(5)′ | 79.00(10) |
| O(10)−Cu(1)−O(2) | 103.81(11) | O(6)−Cu(1)−O(2) | 80.10(11) |
| O(11)−Cu(1)−O(2) | 86.90(11) | O(1)−Cu(1)−O(2) | 85.93(10) |
| O(5)′−Cu(1)−O(2) | 163.78(10) | O(1)−Cu(2)−O(7) | 90.84(12) |
| O(1)″−Cu(2)−O(7) | 89.16(12) | O(8)−Cu(3)−O(1) | 92.33(11) |
| O(8)−Cu(3)−O(1)‴ | 87.67(11) | O(8)−Cu(3)−O(5)″ | 86.42(11) |
| O(1)−Cu(3)−O(5)″ | 103.40(10) | O(8)−Cu(3)−O(5)′ | 93.58(11) |
| O(1)−Cu(3)−O(5)′ | 76.60(10) | | |

[a]Primed atoms generated by the symmetry operation $x + 1, y, z$. Double primed generated by the symmetry operation $-x, -y + 2, -z + 2$. Triple primed generated by the symmetry operation $-x + 1, -y + 2, -z + 2$.

The tapes are supported by the presence of intramolecular hydrogen bonds between the coordinated aqua ligands and the noncoordinated oxygen atoms of the $\mu_4$-sulfate [O(11)···O(3) 2.682, H(11A)···O(3) 1.76 Å, O(11)−H(11A)···O(3) 157°; O(10)···O(4) 2.754, H(10B)···O(4) 1.78 Å, O(10)−H(10B)···O(4) 174°]. There are also intermolecular hydrogen bonds between the tapes that involve the aqua ligands [O(11)···O(4) 2.718, H(11B)···O(4) 1.74 Å, O(11)−H(11B)···O(4) 177°; O(10)···O(3) 2.670, H(10A)···O(3) 1.70 Å, O(10)−H(10A)···O(3) 171°] and these link the tapes into sheets. Furthermore, hydrogen bonds are present between the dimethylammonium cations and the coordinated sulfato oxygen atoms, though notably the hydroxyl O−H group does not act as a hydrogen bond donor.

Although triangular $Cu_3(\mu_3\text{-OH})$ building blocks are relatively well-known in both discrete compounds[19] and polymeric arrays,[16] there are only three previously reported examples of compounds containing $Cu_3(\mu_3\text{-OH})(\mu_3\text{-SO}_4)$ units, in which the second face of the triangle is capped by a sulfato ligand. These are a discrete $Cu_3$ compound that was reported by Beckett and Hoskins in 1972,[20] and two $Cu_{10}(SO_4)_8$ aggregates that were reported more recently.[21,22]

Given the proximity of the $3d^9$ copper(II) centers in **1**−**3**, their magnetic properties are potentially interesting. To explore this, magnetic measurements were undertaken on compounds **1** and **3**. Plots of magnetic susceptibility $\chi T$ against temperature for **1** and **3** in an external magnetic field of 1000 Oe are shown in Figures 5a and 6a, respectively. Both compounds display antiferromagnetic interactions at high temperatures, with the greater temperature dependence observed for **1** suggesting stronger antiferromagnetic interactions in this compound. This result is confirmed by a Curie−Weiss fit to the data above 60 K,


dx.doi.org/10.1021/ic301478x | Inorg. Chem. 2012, 51, 10983−10989

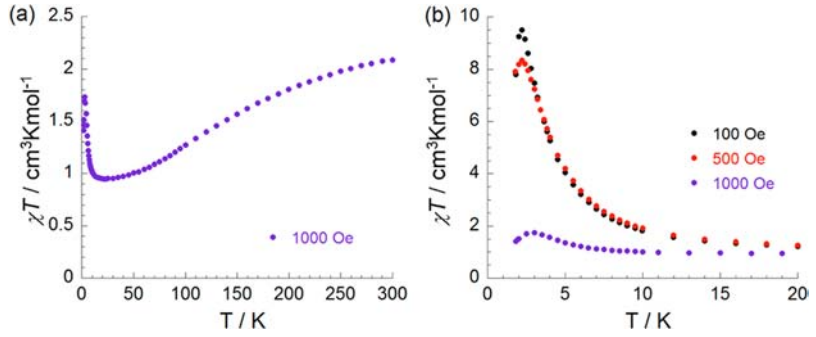


**Figure 5.** Magnetic susceptibility ($\chi T$) vs temperature for $(NMe_2H_2)_4[Cu_6O_2(SO_4)_6(DMF)_4]$ **1** (a) at 1000 Oe and (b) below 20 K for the indicated applied magnetic fields.

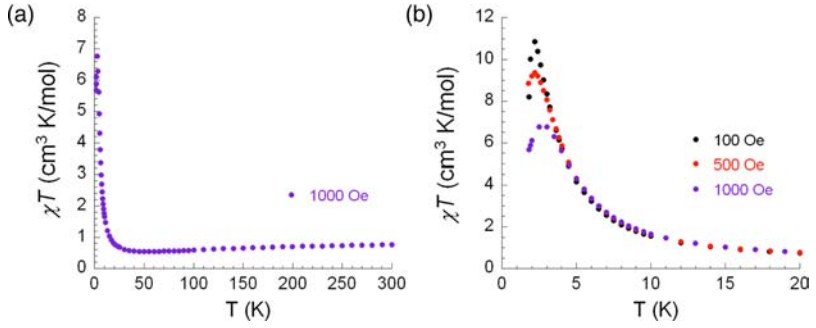


**Figure 6.** Magnetic susceptibility ($\chi T$) vs temperature for $(NMe_2H_2)[Cu_2(OH)(SO_4)_2(H_2O)_2]$ **3** (a) at 1000 Oe and (b) below 20 K for the indicated applied magnetic fields.

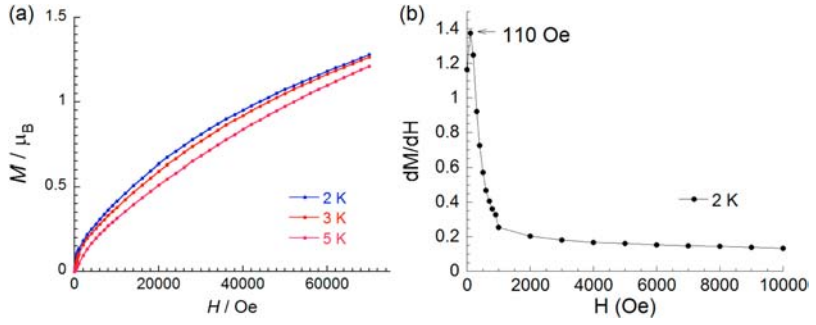


**Figure 7.** Magnetization ($M$) vs external magnetic field ($H$) for $(NMe_2H_2)_4[Cu_6O_2(SO_4)_6(DMF)_4]$ **1** (a) at the indicated temperatures and (b) its first derivative at 2 K showing an inflection point at a field of 110 Oe.

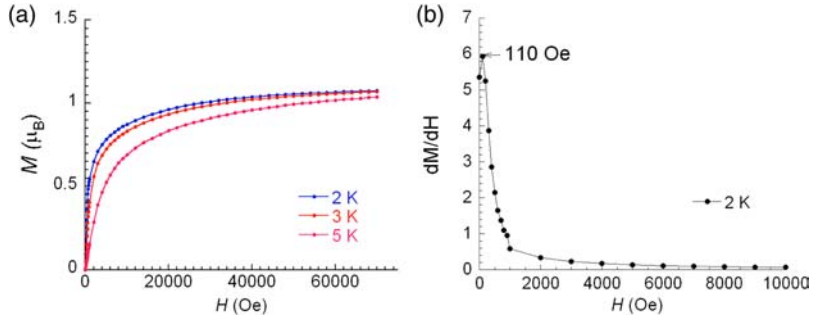


**Figure 8.** Magnetization ($M$) vs external magnetic field ($H$) for $(NMe_2H_2)[Cu_2(OH)(SO_4)_2(H_2O)_2]$ **3** (a) at the indicated temperatures and (b) its first derivative at 2 K showing an inflection point at a field of 110 Oe.

which leads to Weiss constants ($\theta$) of −82.0 and −18.7 K for **1** and **3**, respectively (Supporting Information, Figure S4). Below 20 K (Figures 5b, 6b) the susceptibility $\chi T$ increases rapidly and reaches a maximum at a temperature of approximate 3 K. The maximum value of $\chi T$ increases with the decrease of the external applied magnetic field from 1000 to 100 Oe. This type of field-induced response in the susceptibility is related to the unpaired spins of the $d^9$ copper(II) centers canting to each other at very low temperatures.


dx.doi.org/10.1021/ic301478x | *Inorg. Chem.* 2012, 51, 10983−10989

Magnetization curves for **1** and **3** at temperatures below 5 K (Figures 7a, 8a) reveal that the magnetization, *M*, increases with the external magnetic field, *H*. For **1**, the magnetization increases slowly with *H*, reaching approximately 1.2 $\mu$B at 70 000 Oe though no saturation point was observed. For **3**, the magnetization increases more rapidly and almost reaches a saturation of 1.1 $\mu$B at 70 000 Oe. Derivative plots of the magnetization *M* against external magnetic field *H* are shown in Figures 7b and 8b, respectively. In both cases, metamagnetic behavior is suggested by the presence of an inflection point at a field of 110 Oe, which represents the characteristic field at which the magnetic field overcomes the antiferromagnetic interactions, allowing for parallel alignment of the spins.

AC (alternating current) magnetic susceptibility studies, which monitor the response of a material's magnetic moment to an applied oscillating magnetic field, were also undertaken for the two compounds. The plots of the AC susceptibility in-phase ($\chi'$) component and out-of-phase ($\chi''$) component for both **1** and **3** show the absence of $\chi''$ (Supporting Information, Figure S5, S6) which is probably the result of the small canting angle. Therefore the magnetization is almost canceled when the spin carriers are antiferromagnetically coupled and only slightly canted. Canted antiferromagnetic behavior has been observed previously in copper(II) compounds,[23,24] including the copper-hydroxy-sulfate mineral brochantite, $Cu_4(OH)_6SO_4$.[25]

## CONCLUSIONS

We have prepared three new copper(II) sulfate compounds, in which the anionic charges on the copper-sulfate aggregates are balanced by the presence of dimethylammonium cations derived from either the decomposition of the DMF solvent or addition of $[NMe_2H_2]Cl$. Two of the new compounds, **1** and **2**, contain $Cu_6O_2(SO_4)_6$ aggregates, interconnected by either hydrogen bonding or bridging sulfates, and the only previous report of these aggregates is in the rare copper sulfate mineral fedotovite. The third compound, **3**, has a tape structure in which triangular $Cu_3(OH)(SO_4)$ units share vertices. Magnetic measurements revealed that **1** and **3** are both spin-canting metamagnetic systems, which is similar to the behavior previously observed in some two- and three-dimensional copper(II)-containing networks.[23−26] Field-induced responses were observed below 5 K, with the critical field indicating metamagnetic behavior from antiferromagnetic to ferromagnetic equal to 110 Oe for both compounds.

## ASSOCIATED CONTENT

### Supporting Information

Experimental and simulated powder X-ray diffraction patterns, magnetic measurements, hydrogen bonding distances, and X-ray crystallographic files in CIF format of compounds **1**−**3**. This material is available free of charge via the Internet at http://pubs.acs.org.

## AUTHOR INFORMATION

### Corresponding Author

*E-mail: a.d.burrows@bath.ac.uk. Phone: +44-1225-386529. Fax: +44-1225-386231.

### Notes

The authors declare no competing financial interest.

## ACKNOWLEDGMENTS

The EPSRC is thanked for financial support.

## REFERENCES

(1) Jacobson, A. R.; Dousset, S.; Guichard, N.; Baveye, P.; Andreux, F. *Environ. Pollut.* **2005**, *138*, 250.
(2) Reddy, A.; Ponder, E. L.; Fried, B. *J. Parasitol.* **2004**, *90*, 1332.
(3) Jančula, D.; Maršálek, B. *Chemosphere* **2011**, *85*, 1415.
(4) Wiese, J.; Harris, P.; Bradshaw, D. *Miner. Eng.* **2011**, *24*, 995.
(5) Pluth, J. J.; Steele, I. M.; Kampf, A. R.; Green, D. I. *Mineral. Mag.* **2005**, *69*, 973.
(6) Orlandi, P.; Bonaccorsi, E. *Can. Mineral.* **2009**, *47*, 143.
(7) Hawthorne, F. C.; Ferguson, R. B. *Acta Crystallogr., Sect. B* **1975**, *31*, 1753.
(8) Darling, K.; Ouellette, W.; Prosvirin, A.; Freund, S.; Dunbar, K. R.; Zubieta, J. *Cryst. Growth Des.* **2012**, *12*, 2662.
(9) Basu, C.; Biswas, S.; Chattopadhyay, A. P.; Stoeckli-Evans, H.; Mukherjee, S. *Eur. J. Inorg. Chem.* **2008**, 4927.
(10) Bacchi, A.; Carcelli, M.; Pelizzi, G.; Solinas, C.; Sorace, L. *Inorg. Chim. Acta* **2006**, *359*, 2275.
(11) Li, G.; Xing, Y.; Song, S.; Xu, N.; Liu, X.; Su, Z. *J. Solid State Chem.* **2008**, *181*, 2406.
(12) Lin, J.; Guo, D.-W.; Tian, Y.-Q. *Cryst. Growth Des.* **2008**, *8*, 4571.
(13) Burrows, A. D.; Cassar, K.; Friend, R. M. W.; Mahon, M. F.; Rigby, S. P.; Warren, J. E. *CrystEngComm* **2005**, *7*, 548.
(14) Kraus, W.; Nolzeb, G. *J. Appl. Crystallogr.* **1996**, *29*, 301.
(15) Sheldrick, G. *Acta Crystallogr., Sect. A* **2008**, *64*, 112.
(16) Vilminot, S.; Richard-Plouet, M.; André, G.; Swierczynski, D.; Guillot, M.; Bourée-Vigneron, F.; Drillon, M. *J. Solid State Chem.* **2003**, *170*, 255.
(17) Addison, A. W.; Rao, T. N.; Reedijk, J.; van Rijn, J.; Verschoor, G. C. *J. Chem. Soc., Dalton Trans.* **1984**, 1349.
(18) Starova, G. L.; Filatov, S. K.; Fundamensky, V. S.; Vergasova, L. P. *Mineral. Mag.* **1991**, *55*, 613.
(19) Ferrer, S.; Lloret, F.; Pardo, E.; Clemente-Juan, J. M.; Liu-González, M.; García-Granda, S. *Inorg. Chem.* **2012**, *51*, 985.
(20) Beckett, R.; Hoskins, B. F. *J. Chem. Soc., Dalton Trans.* **1972**, 291.
(21) Wu, J.; Hou, H.-W.; Guo, Y.-X.; Fan, Y.-T.; Wang, X. *Eur. J. Inorg. Chem.* **2009**, 2796.
(22) Pan, F.; Wu, J.; Hou, H.-W.; Fan, Y. *Cryst. Growth Des.* **2010**, *10*, 3835.
(23) Li, J.-R.; Yu, Q.; Sañudo, E. C.; Tao, Y.; Bu, X.-H. *Chem. Commun.* **2007**, 2602.
(24) Guo, L.-R.; Zhu, F.; Chen, Y.; Li, Y.-Z.; Zheng, L.-M. *Dalton Trans.* **2009**, 8548.
(25) Vilminot, S.; Richard-Plouet, M.; André, G.; Swierczynski, D.; Bourée-Vigneron, F.; Kurmoo, M. *Dalton Trans.* **2006**, 1455.
(26) Yang, E.-C.; Liu, Z.-Y.; Wu, X.-Y.; Chang, H.; Wang, E.-C.; Zhao, X.-J. *Dalton Trans.* **2011**, *40*, 10082.